Makale id= 43

Sözlü Sunum

ORCID ID: 0000-0002-4411-411X (M.Terkeş) - 0000-0002-1038-7224 (A.Demirci)

Hibrit Güç Sistemi Fizibilitesinin Batarya Bozulması Dikkate Alınarak Değerlendirilmesi

Arş.Gör. Musa Terkeş[1] , Inst.Öğr. Gör. Dr Alpaslan Demirci[1]
[1]Yıldız Teknik Üniversitesi

Corresponding author: Musa Terkeş

Özet: *Enerjide yenilenebilir teknolojilerin yaygınlaştırılması karbon hedefleri açısından değerlidir. Ancak, kesintili enerji üretim profili nedeniyle, sistemin üstün batarya enerji depolama sistemleri (BESS) ile desteklenmesi ve hibrit güç sistemlerinin (HPS) tasarlanması, güvenilir ve sürdürülebilir bir enerji arzı için kritik öneme sahiptir. BESS'in teknik çalışması, enerji dengesini ve sistem performansını birçok açıdan etkileyebilir. Bu çalışmada, minimum maliyetli HPS'ler, düşük deşarj derinliklerinde (DOD) paylaşılan BESS kullanılarak dağıtım şebekesindeki tüketici talepleri için çok yıllı bir duyarlılık analizinde optimum şekilde boyutlandırılmıştır. Buna ek olarak, düşük DOD'nin neden olduğu HPS fizibilite sonuçları, çeşitli C oranı ve değiştirme bozulma limitleri dikkate alınarak iyileştirilmiştir. Sonuçlar, C oranının artırılmasının enerji maliyetini %3,15'e kadar ve CO2'yi %8,9'a kadar azaltabileceğini göstermektedir. Ayrıca, değişime kadarki bozulma limitlerinin %30'a kadar azaltılması, toplam net bugünkü maliyetleri %5,63'e kadar düşürebilir ve yenilenebilir oranı %1,1'e kadar artırabilir. BESS'in teknik işleyişinin birçok paydaşın bakış açısından değerlendirilmesi, sürdürülebilir kalkınma planlarına yardımcı olacaktır.*

Anahtar Kelimeler: *Batarya Bozulması, C Oranı, Deşarj Derinliği, Optimizasyon, Hibrit Güç Sistemleri*

Evaluation of Hybrid Power System Feasibility Considering Battery Degradation

Abstract: *The deployment of renewable technologies in energy is valuable for carbon targets. However, due to their intermittent power generation profile, supporting the system with superior battery energy storage systems (BESS) and designing hybrid power systems (HPS) is critical for a reliable and sustainable energy supply. The technical operation of BESS can affect the energy balance and system performance in many aspects. In this study, minimum cost HPSs are optimally sized in a multi-year sensitivity analysis for prosumer demands in the distribution grid using shared BESS at lower depths of discharge (DOD). In addition, the HPS feasibility results caused by low DOD are improved by considering various C-rate and replacement degradation limits. The results show that increasing the C-rate can reduce the cost of energy by up to 3.15% and CO2 by up to 8.9%. Moreover, reducing replacement degradation limits by up to 30% could lower total net present costs by up to 5.63% and increase the renewable fraction by up to 1.1%. Evaluating the technical operation of BESS from the perspective of many stakeholders will help sustainable development plans.*

Keywords: *Battery Degradation, C-Rate, Depth of Discharge, Optimization, Hybrid Power Systems*

1. INTRODUCTION

The performance of batteries is tightly coupled to charge and discharge cycles that gradually reduce their capacity. In addition, a higher C-rate cause the voltage to drop rapidly due to the greater internal resistance (Kebede et al., 2021). To balance economics and state of health (SOH) at the utility-scale, transforming variable high C-rate and battery efficiencies into economic representations in an optimization framework can increase revenues (Sarker et al., 2017). However, especially in radial

distribution grids, extremely high penetration of distributed energy resources (DERs) and increased grid dependency can lead to reverse power flow. To avoid this problem, improving the voltage profile and reducing the active power loss is necessary, considering the effect of C-rates for the optimal placement and sizing of battery energy storage systems (BESS) (Gupta et al., 2022a). In particular, a C-rate of 0.33 can guarantee reliable operation compared to others (Gupta et al., 2022b).

Differently, in the transition to zero-energy buildings, the depreciation of the initial investment, self-consumption rate, feed-in rate, simultaneity in energy generation and consumption, and the effects of depth of discharge (DOD) and discharge power on SOH complicate the BESS sizing process (Tsioumas et al., 2021). Moreover, the trade-off between BESS investment costs and lifetime to determine the optimal DODs is one of the critical issues in the microgrid integration of BESS (Wu et al., 2022). Solving the complex charge/discharge schedules and the trade-off between DOD and BESS lifetime can solve these issues, minimizing the cost of microgrid extensions in short and long-term operational plans (Alsaidan et al., 2016). However, the four classical single-factor-based battery degradation models (Arrhenius, CAPN, linear, and PLET) can also impact day-ahead energy management strategies in the microgrid (Wang et al., 2020). Arrhenius models determine battery life as a function of temperature, C-rate, SOH, and aging and help to accurately estimate cycle life (Kucinskis et al., 2022). For optimal BESS sizing toward renewable energy integration, such models may also need to consider the aging characteristics of the technology and the power profile that the system may confront (De La Torre et al., 2019). Moreover, including additional costs due to battery degradation in optimal management plans strengthens the correlation of different operating models with degradation costs (Bordin et al., 2017). In contrast to Arrhenius, neural network estimation of battery degradation based on ambient temperature, C-rate, state of charge (SOC), DOD, and available energy capacity can reduce battery system cost by up to 78.6% in microgrids using the day-ahead market (Zhao & Li, 2023). Also, ensuring optimum degradation characteristics under operating conditions can minimize annual storage costs in DC microgrids (Dulout et al., 2017).

On the other hand, using batteries in stationary energy storage systems (ESS) without considering degradation can increase the renewable fraction (RF) by up to 20.25% (Zieba Falama et al., 2022), load coverage and self-consumption by up to 14.08% and 16.56% (Liu et al., 2020). This neglect could also reduce the usage of diesel generators and COE by 1.3% (Jacobus et al., 2011) and 28% (Qi et al., 2022) and thus eliminate CO_2 by 3.62% (Üçtuğ & Azapagic, 2018). Although benefits can be maximized without considering battery degradation in hybrid power systems (HPSs), inaccurate results will risk operational plans. However, in many application areas, such as peak demand reduction, control reserve, and UPS, it is critical to consider the BESS based on different stress levels and degradation probabilities, including the operating time and mode (Kraenzl et al., 2019). Differently, to incorporate wind energy into frequency modulation, the shortcomings of existing DOD-based models in linearization problems need to be addressed with C-rate approaches that consider different control methods of BESS (Qiu et al., 2022). The performance degradation of BESSs under different storage and cycling conditions depending on their thermal environment and charge-discharge routines should also be characterized to smooth renewable energy generation profiles (Smith et al., 2017). Moreover, in off-grid systems, determining the energy supply from the BESS and the load demand during charge-discharge cycles at the lowest cost and with high reliability can guarantee the battery degradation cost and optimal DOD (Hlal et al., 2019). However, operating all cycles at different DODs and optimal SOCs for each day can provide a reliable feasibility process (Fallahifar & Kalantar, 2023). In addition, determining suitable BESS control strategies based on functionality and power capacity reduces lifecycle costs and increases self-sufficiency rates (Shabani et al., 2021). Although worthwhile, the effects of capacity decay and temperature variation must be carefully considered in BESSs and control strategies to determine renewable energy capacity factors (Jung et al., 2020). Charging BESSs, especially in the case of wind power curtailment, is critical to the sustainability of utility-level energy services (Rayit et al., 2021).

The effects of various degradation parameters have been frequently tested and evaluated in many literature studies. However, this study evaluates degradation parameters in simultaneously developed aging models considering Arrhenius-based functional, relative capacity versus temperature, cycle to failure versus DOD, and life versus temperature curves. In addition, the Rainflow counting algorithm is used to analyze aging based on cycles and calendar degradation. Moreover, C-rate and replacement

degradation limit effects are evaluated to improve battery aging performance at lower DODs. The benefits in technical, economic, and environmental optimization outputs in the developed HPS model are compared. Also, increasing electricity tariff, electricity demand, and PV degradation are considered in multi-year in-depth sensitivity analyses to enhance the accuracy of the minimum cost optimal HPS feasibility outputs for the prosumer distribution network using shared common BESS.

2. METHODOLOGY

2.1. HPS Design and Modeling

In this study, the PV model is represented by three different equations. The PV array output power is calculated by Equation (1), while the cell temperatures are determined by Equation (2) to be used in Equation (1). The efficiency that the PV model can provide under nominal test conditions is considered by Equation (3).

$$P_{PV}(t) = Y_{PV}.f_{PV}.\left(\frac{G_T(t)}{G_{T,STC}}\right).\left[1+\alpha_P.\left(T_C(t)-T_{C,STC}\right)\right] \quad (1)$$

$$T_C(t) = T_a(t) + \frac{G_T(t)}{800}.(T_{NOCT}-20) \quad (2)$$

$$\eta_{mp,STC} = \frac{Y_{PV}}{A_{PV}.G_{T,STC}} \quad (3)$$

Three parameters for the storage system modeled with a two-tank system, chemically bound energy, and available energy for energy conversion are considered. The first is the maximum storage capacity, which indicates the total energy the two tanks can store. The second is the capacity ratio, which is the ratio of the size of the available energy to the composite size of both tanks. Finally, the rate constant is the energy conversion rate from bound energy to available energy or vice versa. Based on these parameters, the maximum power that the tank can charge over a given period is determined by Equation (4) and its discharge by Equation (5). In the case of discharge efficiency, the maximum discharge power is calculated by Equation (6). In addition to determining the range of energy entering and leaving the storage bank, two limitations are imposed on the maximum charging power. The first one corresponds to the maximum charging rate at which the charging power of the storage is calculated by Equation (7). Another limitation is related to the maximum charging current and is calculated by Equation (8). In particular, considering the three limitations on the charging power and the charging efficiency of the storage, the maximum charging power is set to the lowest value in Equation (9). After calculating the actual charging or discharging power at each time step, HOMER calculates the bound energy obtained with Equation (10) and the available energy with Equation (11). In addition, the lifetime energy output of the battery pack is calculated in Equation (12) depending on the maximum capacity and voltage of the storage, the number of cycles until the change, and the DOD.

$$P_{batt,cmax,kbm} = \frac{kQ_1e^{-k\Delta t} + Qkc(1-e^{-k\Delta t})}{1-e^{-k\Delta t}+c(k\Delta t-1+e^{-k\Delta t})} \quad (4)$$

$$P_{batt,dmax,kbm} = \frac{-kcQ_{max} + kQ_1e^{-k\Delta t} + Qkc(1-e^{-k\Delta t})}{1-e^{-k\Delta t}+c(k\Delta t-1+e^{-k\Delta t})} \quad (5)$$

$$P_{batt,dmax} = P_{batt,dmax,kbm}\eta_{batt,d} \quad (6)$$

$$P_{batt,cmax,mcr} = \frac{(1-e^{-\alpha_c\Delta t})(Q_{max}-Q)}{\Delta t} \quad (7)$$

$$P_{batt,cmax,mcc} = \frac{N_{batt}I_{max}V_{nom}}{1000} \quad (8)$$

$$P_{batt,cmax} = \frac{MIN\left(P_{batt,cmax,kbm}\,,\,P_{batt,cmax,mcr}\,,\,P_{batt,cmax,mcc}\right)}{\eta_{batt,c}} \quad (9)$$

$$Q_{1,end} = Q_1e^{-k\Delta t} + \frac{(kcQ-P)(1-e^{-k\Delta t})}{k} + \frac{Pc(k\Delta t-1+e^{-k\Delta t})}{k} \quad (10)$$

$$Q_{2,end} = Q_2 e^{-k\Delta t} + Q(1-c)(1-e^{-k\Delta t}) + \frac{P(1-c)(k\Delta t - 1 + e^{-k\Delta t})}{k} \quad (11)$$

$$Q_{lifetime} = f_i d_i \left(\frac{q_{max} V_{nom}}{1000\, W/kW}\right) \quad (12)$$

The first sub-model of the aging model uses the functional approach. Based on the battery's internal resistance, it is possible to consider the losses and calculate the output power using Equation (13). Depending on the circuit behavior and considering the square of the circuit current, the output power decreases with increasing current. By equalizing the derivative of the output power about the circuit current to zero, the limitation to the maximum current corresponding to the maximum output power is given by Equation (14).

$$P_{out} = V_0 I - R_0 I^2 \quad (13)$$

$$I_{Pout,max} = \frac{V_0}{2R_0} \quad (14)$$

Another of the sub-models involves characterizing the temperature as the bulk thermal capacity. At each time step of the simulation, the energy dissipated by the active series resistor is either converted into heat or increases the bulk temperature in the storage bank. The corresponding heat is transferred to or removed from the ambient according to the convection equation (q=hΔt). The thermal energy lost due to series resistance is calculated by Equation (15). At the same time, the rate of change in the internal temperature of the battery acts according to the energy balance Equation (16). The differential solution of the energy balance equation is determined by Equation (17). Based on the relevant equations, HOMER effectively adjusts the SOC_{min} depending on the available temperature of the battery pack.

$$\dot{Q} = I^2 R \quad (15)$$

$$mc\dot{T} = \dot{Q} - (T - T_a)h \quad (16)$$

$$T_{i+1} = \left(T_i - T_a - \frac{\dot{Q}}{h}\right) e^{-\frac{h}{mc}dt} + \frac{\dot{Q}}{h} + T_a \quad (17)$$

The relative capacity concerning temperature represents another sub-model and is calculated in Equation (18) by fitting the parameters d_0, d_1, and d_2 promised by battery manufacturers.

$$Capacity(T) = Nominal\, Capacity.(d_0 + d_1 T + d_2 T^2) \quad (18)$$

The most important of the sub-models is how to calculate calendar and cycle aging. Functional degradation is considered as a capacity reduction and series resistance increase. Increasing degradation rates at each time step, regardless of whether the tank is in use or idle, are determined in calendar aging. Calendar aging depends only on temperature, as in Equation (19). In contrast, cycle aging refers to the cycle fatigue in the battery. The number of DOD-dependent cycles until replacement is calculated by Equation (20). The rainflow counting algorithm converts the SOC-dependent time series into discrete cycles with each DOD. In contrast, the cumulative cycle degradation is calculated from the DOD associated with each cycle with Equation (21).

$$kt = Be^{-\frac{d}{T}} \quad (19)$$

$$1/N = AD^{\beta} \quad (20)$$

$$D = \sum_{i=0}^{N} AD_i^{\beta} \quad (21)$$

AC to DC and DC to AC energy conversion is provided by a converter that can operate as an inverter and a rectifier. Inverter output power is calculated in Equation (22), rectifier output power in Equation (23), and converter efficiency in Equation (24).

$$P_{inv}(t) = \eta_{inv} . P_{DC}(t) \quad (22)$$

$$P_{rec}(t) = \eta_{rec} \cdot P_{AC}(t) \quad (23)$$

$$\eta_{DC/AC} = \frac{P_{PV}}{P_{Converter}} \quad (24)$$

The PV, BESS, and converter meet the demand of 30 household prosumers connected to the common distribution busbar, each consuming 10 kWh of energy daily. At the same time, energy is also purchased from the grid, considering the intermittency of renewable energy sources and the fully discharged BESS. On the other hand, the residual energy is sold to the grid at 0.02 $/kWh. The study was conducted in Istanbul, considering the time-of-use (TOU) grid tariff. Although a carbon tax has not yet been introduced, the impact of a unit of electricity purchased from the grid on carbon emissions is calculated as 426.1 g/kWh when considering a carbon tax of 20 $/ton as a future projection. Differently, an inflation rate of 14%, a nominal discount rate of 23.3%, and a project lifetime of 20 years are assumed. In addition, multi-year sensitivity analyses were performed in HOMER Pro, considering an electricity tariff of 3.5%, electricity demand of 2.3%, and PV degradation of 0.5%. The HPS model is shown in **Error! Reference source not found.**, while the technical and economic optimization inputs of the HPS are given in

Table **20**.

Figure 15. HPS Model

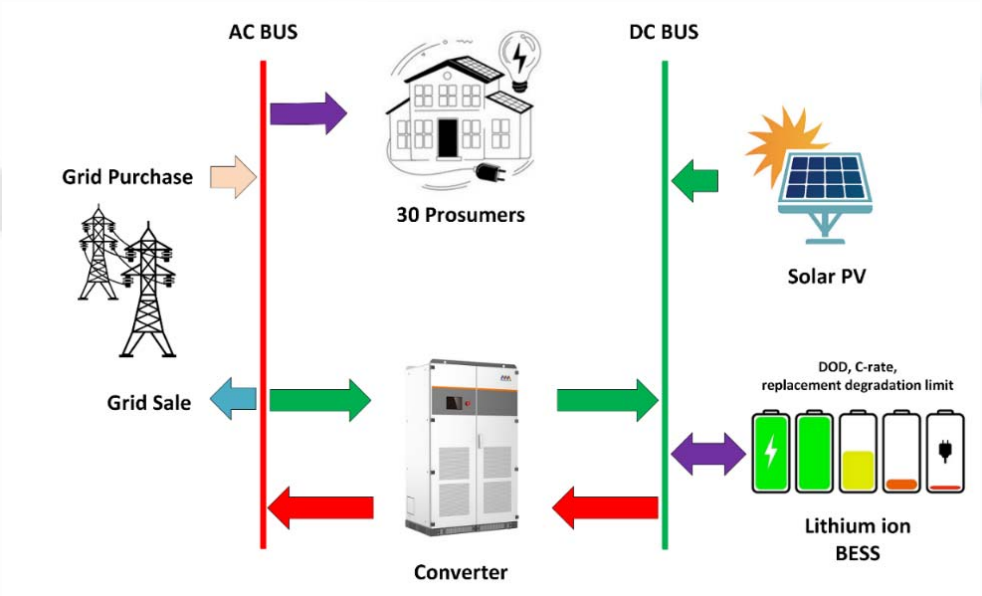


Table 20. Optimization Inputs

HPS	Parameter description		
PV	Capital cost	1500	$/kW
	Replacement cost	1250	$/kW
	O&M cost	10	$/kW/yr
Converter	Capital cost	300	$/kW
	Replacement cost	300	$/kW
	O&M cost	0	$/kW/yr
BESS	Capital cost	300	$/kWh

HPS	Parameter description		
	Replacement cost	250	$/kWh
	O&M cost	5	$/kWh/yr
Load	Peak load	61.76	kW
	Average energy consumption	300	kWh/day
	Load factor	20	%
Grid	Flat tariff (06.00-17.00)	0.0822	$/kWh
	Peak tariff (17.00-22.00)	0.1199	$/kWh
	Valley tariff (22.00-06.00)	0.052	$/kWh

2.2. Scenarios of the Study

This study focuses on enhancing the technical, economic, and environmental HPS feasibility outputs in case of operating at lower DOD and improving the performance concerning BESS aging while considering the C-rate and replacement degradation limit for the relevant objective. In the HOMER optimization framework, the optimal sizing is performed with a minimum cost objective, and to robustly assess the possible impact of the C-rate due to lower DOD, the maximum useful capacities are assumed to be 300 kW for PV, 250 kWh for ESS and 200 kW for converter. The scenarios considered in the study are shown in Table 21.

Table 21. Scenarios of the Study

Scenarios	PV Capacity (kW)	BESS (kWh)	Converter Capacity (kW)	DOD_{max} (%)	C-rate	Replacement degradation limit (%)
A	300	250	200	50	0.2-3 C	50
B						20

2.3. Objective Functions and Decision Criteria

NPC minimization is performed in coordination with COE, and hybrid configurations with many possible costs are presented to stakeholders in an incremental financial order on the optimization screen. The difference between financial cash flows and revenues at the end of each year is discounted to a present-day basis and summed. Accordingly, NPC is calculated by Equation (25), while the capital recovery factor (CRF) used in the NPC calculation is determined by Equation (26) depending on the discount rate and project lifetime. On the other hand, COE is calculated by Equation (27) as the ratio of annual electricity generation cost to the electricity load served, while operating costs are determined by Equation (28).

$$NPC = \frac{\frac{Total\ annual\ cost\ of\ HPS}{CRF}}{\frac{i(1+i)^N}{(1+i)^N - 1}} \tag{25}$$

$$CRF(i,N) = \frac{i\ .\ (1+i)^n}{i\ .\ (1+i) - 1} \tag{26}$$

$$COE = \frac{CRF\left(i, R_{proj}\right)NPC}{E_{Served}} \tag{27}$$

$$C_{operating} = CRF\left(i, R_{proj}\right)NPC - C_{ann,cap} \tag{28}$$

The other objectives of the study are to ensure that the RF is as high as possible and that the total carbon emissions are as low as possible. Accordingly, how much electricity demand can be met from renewable energy is calculated in Equation (29). At the same time, cumulative CO_2 is determined in Equation (30) based on the emission factor per unit of electricity in the grid mix.

$$RF = \left(1 - \frac{E_{non-ren.}}{E_{load}}\right) 100 \tag{29}$$

$$TCO_2 = \sum_{t=1}^{N} (CO_2)_t \left(EF_{grid}\right)_t \tag{30}$$

The other critical criteria for the BESS technique are battery wear cost and autonomy. The storage wear cost, which represents the energy cycle cost in $/kWh, is calculated in Equation (31), while the autonomy, known as the size of the storage bank with respect to the electrical load, is evaluated in Equation (32).

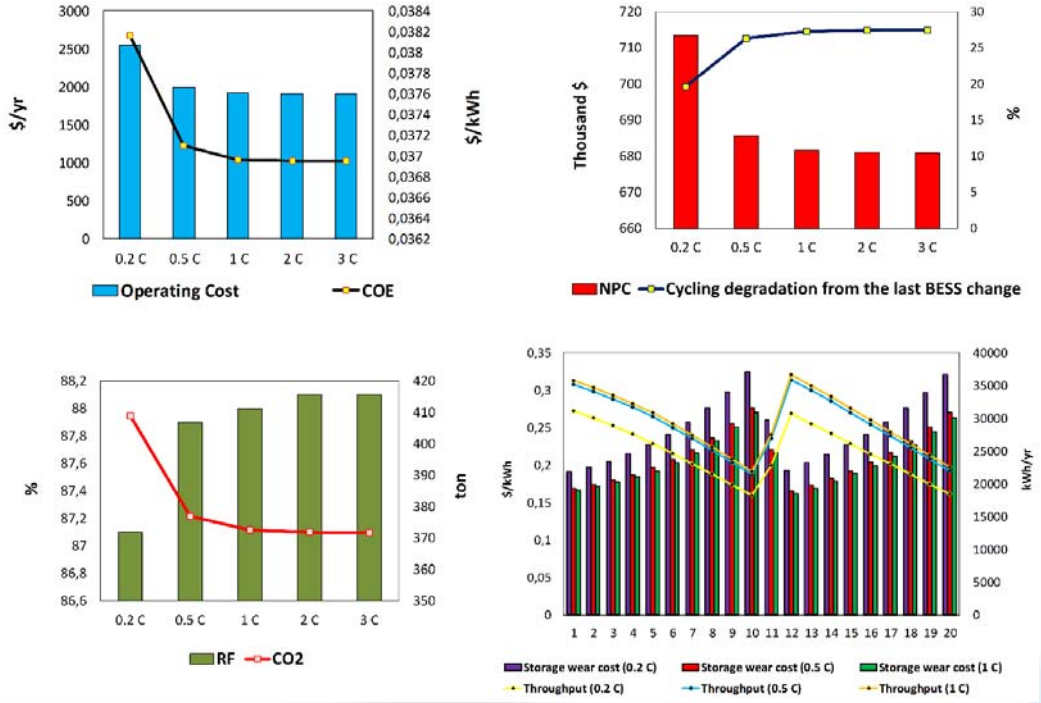
$$C_{bw} = \frac{C_{rep,batt}}{N_{batt} Q_{lifetime} \sqrt{\eta_{rt}}} \tag{31}$$

$$Autonomy = \frac{N_{batt} V_{nom} Q_{nom} \left(1 - \frac{q_{min}}{100}\right) (24\ h/d)}{L_{prim,ave} (1000\ Wh/kWh)} \tag{32}$$

3. OPTIMIZATION RESULTS

Figure **16** shows the impact of the C-rate on HPS outputs, including operating cost, COE, NPC, RF, RF, CO_2, storage wear cost, throughput, and cycle degradation. In general, C-rates above 1 C have little impact on HPS outputs. The increase in charging and discharging currents and powers makes BESS more valuable in meeting prosumer demand and better utilization of PV power generation. COE can be reduced by up to 3.15% and NPC by up to 4.46% due to the improved performance in the supply-demand balance. As the total operating cost of the system is not only dependent on BESS and due to the improved performance in energy management, annual operating costs are reduced by up to 24.78% on average, and many prosumer benefits such as selling electricity to the grid are realized. Moreover, increases in C-rates towards carbon neutrality targets reduced CO_2 by up to 8.9% and increased RF by up to 1%, even for a small operation scale in the study. However, due to the higher charging and discharging currents and powers, the cycle degradation until BESS replacement increases to 7.82%, and the associated trade-off must be considered.

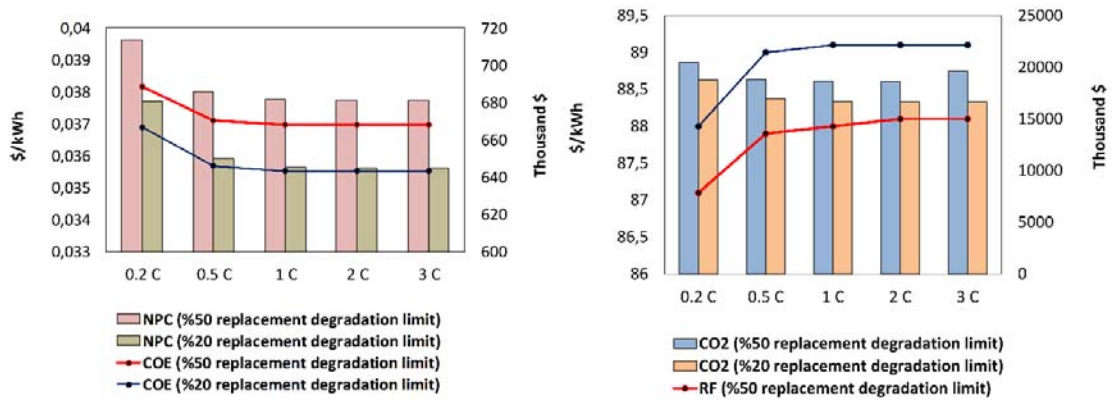
Figure 16. HPS Feasibility Depending on C-rate



On the contrary, at higher C-rates, with a replacement degradation limit of 20%, COE can be reduced by up to 3.69%, NPC by up to 5.2%, and RF by up to 1.1%. CO_2 is eliminated by up to 11.15%, while total annual operating costs are reduced by 37.35%. Accordingly, the comparative effect of the C-rate and the 20% and 50% replacement degradation limit on the system is shown in

Figure **17**. Lowering the replacement degradation limit can maximize prosumer benefits. For example, compared to Scenario A at lower C rates, COE can be reduced by up to 3.35%, NPC by up to 4.63%, CO_2 by up to 8.16%, and operating costs by up to 25.4%. At higher C rates, these benefits can be increased by up to 1% for COE and NPC, up to 2.3% for CO_2, and up to 12.5% for operating costs. In this context, higher C-rates emphasize the difference between the effects of replacement degradation limits on HPS outputs.

Figure 17. The Effect of Replacement Degradation Limit on HPS Feasibility Considering C-rate



4. CONCLUSIONS

This study proposes a minimum cost optimum HPS for a prosumer distribution network using shared common storage. At the same time, the reduction in technical, economic, and environmental parameters

due to the operation of BESS at lower DOD is improved by considering the C-rate and replacement degradation limit. Moreover, multi-year sensitivity analysis considers four different sub-degradation models, cumulative increasing electricity demand, grid tariff, and PV degradation: Functional, relative capacity versus temperature, cycle to failure versus DOD, and lifetime curves versus temperature using Arrhenius and Rainflow counting methods. The results show that increasing C-rates can reduce COE by up to 3.15% and CO_2 by up to 8.9% under a higher replacement degradation limit. However, an increase of up to 7.82% in cycle degradation up to the BESS replacement could cause a trade-off situation. On the other hand, lowering the replacement degradation limit can reduce NPC by up to 5.63% and CO_2 by up to 10.46% while increasing RF by up to 1.1%. According to the results, the significant beneficial impacts on C-rate and replacement degradation limits, even at small operating scales, can bring many stakeholders together in a win-win environment for carbon neutrality goals. Additionally, this study can be extended to green policies using different battery technologies, considering various discharge depths and hourly and daily demand variability.

5. References

[1] Alsaidan, I., Khodaei, A., & Gao, W. (2016). Determination of optimal size and depth of discharge for battery energy storage in standalone microgrids. *NAPS 2016 - 48th North American Power Symposium, Proceedings*, 1–6. https://doi.org/10.1109/NAPS.2016.7747845

[2] Bordin, C., Anuta, H. O., Crossland, A., Gutierrez, I. L., Dent, C. J., & Vigo, D. (2017). A linear programming approach for battery degradation analysis and optimization in offgrid power systems with solar energy integration. *Renewable Energy*, *101*, 417–430. https://doi.org/10.1016/j.renene.2016.08.066

[3] De La Torre, S., González-González, J. M., Aguado, J. A., & Martín, S. (2019). Optimal battery sizing considering degradation for renewable energy integration. *IET Renewable Power Generation*, *13*(4), 572–577. https://doi.org/10.1049/iet-rpg.2018.5489

[4] Dulout, J., Jammes, B., Alonso, C., Anvari-Moghaddam, A., Luna, A., & Guerrero, J. M. (2017). Optimal sizing of a lithium battery energy storage system for grid-connected photovoltaic systems. *2017 IEEE 2nd International Conference on Direct Current Microgrids, ICDCM 2017*, *1*, 582–587. https://doi.org/10.1109/ICDCM.2017.8001106

[5] Fallahifar, R., & Kalantar, M. (2023). Optimal planning of lithium ion battery energy storage for microgrid applications: Considering capacity degradation. *Journal of Energy Storage*, *57*(December 2022), 106103. https://doi.org/10.1016/j.est.2022.106103

[6] Gupta, S., Rawat, M. S., & Gupta, T. N. (2022a). Optimal Placement and Sizing of Various C-Rate Type of BESS for Minimizing Reverse Power Flow in Radial Distribution Network. *2022 2nd International Conference on Emerging Frontiers in Electrical and Electronic Technologies, ICEFEET 2022*, 1–6. https://doi.org/10.1109/ICEFEET51821.2022.9847772

[7] Gupta, S., Rawat, M. S., & Gupta, T. N. (2022b). Optimal Placement and Sizing of Various C-Rate Type of BESS for Minimizing the Impact of Intermittent DG Output on Hourly Peak Load Variation in Radial Distribution Network. *2022 2nd International Conference on Emerging Frontiers in Electrical and Electronic Technologies, ICEFEET 2022*, 1–6. https://doi.org/10.1109/ICEFEET51821.2022.9847777

[8] Hlal, M. I., Ramachandaramurthy, V. K., Sarhan, A., Pouryekta, A., & Subramaniam, U. (2019). Optimum battery depth of discharge for off-grid solar PV/battery system. *Journal of Energy Storage*, *26*(June), 100999. https://doi.org/10.1016/j.est.2019.100999

[9] Jacobus, H., Lin, B., Jimmy, D. H., Ansumana, R., Malanoski, A. P., & Stenger, D. (2011). Evaluating the impact of adding energy storage on the performance of a hybrid power system. *Energy Conversion and Management*, *52*(7), 2604–2610. https://doi.org/10.1016/j.enconman.2011.01.015

[10] Jung, W., Jeong, J., Kim, J., & Chang, D. (2020). Optimization of hybrid off-grid system consisting of renewables and Li-ion batteries. *Journal of Power Sources*, *451*(January), 227754. https://doi.org/10.1016/j.jpowsour.2020.227754

[11] Kebede, A. A., Coosemans, T., Messagie, M., Jemal, T., Behabtu, H. A., Van Mierlo, J., & Berecibar, M. (2021). Techno-economic analysis of lithium-ion and lead-acid batteries in stationary energy storage application. *Journal of Energy Storage*, *40*(November 2020), 102748. https://doi.org/10.1016/j.est.2021.102748

[12] Kraenzl, J., Nguyen, T. T., & Jossen, A. (2019). Investigating stationary storage applications and their impact on battery aging. *2019 14th International Conference on Ecological Vehicles and Renewable Energies, EVER 2019*, 1–9. https://doi.org/10.1109/EVER.2019.8813636

[13] Kucinskis, G., Bozorgchenani, M., Feinauer, M., Kasper, M., Wohlfahrt-Mehrens, M., & Waldmann, T. (2022). Arrhenius plots for Li-ion battery ageing as a function of temperature, C-rate, and ageing state – An experimental study. *Journal of Power Sources*, *549*(June), 232129. https://doi.org/10.1016/j.jpowsour.2022.232129

[14] Liu, J., Wang, M., Peng, J., Chen, X., Cao, S., & Yang, H. (2020). Techno-economic design optimization of hybrid renewable energy applications for high-rise residential buildings. *Energy Conversion and Management*, *213*(March), 112868. https://doi.org/10.1016/j.enconman.2020.112868

[15] Qi, X., Wang, J., Królczyk, G., Gardoni, P., & Li, Z. (2022). Sustainability analysis of a hybrid renewable power system with battery storage for islands application. *Journal of Energy Storage*, *50*(March). https://doi.org/10.1016/j.est.2022.104682

[16] Qiu, Z., Zhang, W., Lu, S., Li, C., Wang, J., Meng, K., & Dong, Z. (2022). Charging-rate-based Battery Energy Storage System in Wind Farm and Battery Storage Cooperation Bidding Problem. *CSEE Journal of Power and Energy Systems*, *8*(3), 659–668. https://doi.org/10.17775/CSEEJPES.2021.00230

[17] Rayit, N. S., Chowdhury, J. I., & Balta-Ozkan, N. (2021). Techno-economic optimisation of battery storage for grid-level energy services using curtailed energy from wind. *Journal of Energy Storage*, *39*(April), 102641. https://doi.org/10.1016/j.est.2021.102641

[18] Sarker, M. R., Murbach, M. D., Schwartz, D. T., & Ortega-Vazquez, M. A. (2017). Optimal operation of a battery energy storage system: Trade-off between grid economics and storage health. *Electric Power Systems Research*, *152*, 342–349. https://doi.org/10.1016/j.epsr.2017.07.007

[19] Shabani, M., Dahlquist, E., Wallin, F., & Yan, J. (2021). Techno-economic impacts of battery performance models and control strategies on optimal design of a grid-connected PV system. *Energy Conversion and Management*, *245*(June), 114617. https://doi.org/10.1016/j.enconman.2021.114617

[20] Smith, K., Saxon, A., Keyser, M., Lundstrom, B., Cao, Z., & Roc, A. (2017). Life prediction model for grid-connected Li-ion battery energy storage system. *Proceedings of the American Control Conference*, 4062–4068. https://doi.org/10.23919/ACC.2017.7963578

[21] Tsioumas, E., Jabbour, N., Koseoglou, M., Papagiannis, D., & Mademlis, C. (2021). Enhanced Sizing Methodology for the Renewable Energy Sources and the Battery Storage System in a Nearly Zero Energy Building. *IEEE Transactions on Power Electronics*, *36*(9), 10142–10156. https://doi.org/10.1109/TPEL.2021.3058395

[22] Üçtuğ, F. G., & Azapagic, A. (2018). Environmental impacts of small-scale hybrid energy systems: Coupling solar photovoltaics and lithium-ion batteries. *Science of the Total Environment*, *643*, 1579–1589. https://doi.org/10.1016/j.scitotenv.2018.06.290

[23] Wang, S., Guo, D., Han, X., Lu, L., Sun, K., Li, W., Sauer, D. U., & Ouyang, M. (2020). Impact of battery degradation models on energy management of a grid-connected DC microgrid. *Energy*, *207*, 118228. https://doi.org/10.1016/j.energy.2020.118228

[24] Wu, Y., Liu, Z., Liu, J., Xiao, H., Liu, R., & Zhang, L. (2022). Optimal battery capacity of grid-connected PV-battery systems considering battery degradation. *Renewable Energy*, *181*, 10–23. https://doi.org/10.1016/j.renene.2021.09.036

[25] Zhao, C., & Li, X. (2023). Microgrid Optimal Energy Scheduling Considering Neural Network based Battery Degradation. *IEEE Transactions on Power Systems*, *PP*, 1–12. https://doi.org/10.1109/tpwrs.2023.3239113

[26] Zieba Falama, R., Dawoua Kaoutoing, M., Kwefeu Mbakop, F., Dumbrava, V., Makloufi, S., Djongyang, N., Salah, C. Ben, & Doka, S. Y. (2022). A comparative study based on a techno-environmental-economic analysis of some hybrid grid-connected systems operating under electricity blackouts: A case study in Cameroon. *Energy Conversion and Management*, *251*(October 2021), 114935. https://doi.org/10.1016/j.enconman.2021.114935